Astron. Astrophys. 342, 763–772 (1999)

ASTRONOMY
AND
ASTROPHYSICS

Derivation of veiling, visual extinction and excess flux from spectra of T Tauri stars

A. Chelli

Laboratoire d'Astrophysique, Observatoire de Grenoble, U.J.F./B.P. 53, F-38041 Grenoble Cedex 9, France

Received 29 December 1997 / Accepted 27 October 1998

Abstract. This work aims to analyse within a rigorous framework, veiling, visual extinction and excess extraction from the spectra of T Tauri stars. We investigate further the method of Hartigan et al. (1989) for veiling estimate from small spectral bandwidth of a few tens of Angstroms. The calculated veiling value is sensitive to the estimated noise ratio and to spectral mismatches between the object and the reference. We show that an incorrect input noise ratio together with low contrast spectra in noise units can lead to important biasses and we propose solutions to minimize this problem. In case of spectral mismatches and for large contrast spectra compared to the residual of the veiling equation, the relative veiling bias is dominated by the apparent veiling of the reference with respect to the correct underlying object stellar spectrum. The veiling error is found to be proportional to the square of the veiling when the latter becomes larger than unity. If we are limited by the statistical noise, it is little dependent on the spectral resolution. Because of systematic errors, however, it will be difficult to estimate the veiling in a very small bandwidth at spectral resolutions of a few hundreds.

For visual extinction and excess estimates, we generalize the discrete method of Gullbring et al. (1998) by a continuous approach. This new approach, which uses the spectra as a whole through a continuous modelling, has been successfully tested on simulated data. The visual extinction error is proportional to the veiling when the veiling becomes larger than unity and to a function which depends on the input reference spectrum. This function decreases with increasing spectrum contrast, which means going from earlier to later spectral types. If we are limited by the statistical noise, it is, like the veiling, little dependent on the spectral resolution. For very active T Tauri stars or when the excess is dominated by emission lines, however, it will be difficult to handle very low spectral resolutions, because of systematic errors. The real sensitivity to biasses and the performances of the algorithm are to be studied experimentally. Nevertheless, an efficient use of all the information contained in the spectra through the proposed "continuous" approach, together with a better understanding of the sources of bias, can greatly help to derive the visual extinction and the excess on objects much fainter than those so far studied.

Send offprint requests to: A. Chelli

Key words: methods: data analysis – techniques: spectroscopic – stars: circumstellar matter – stars: pre-main sequence

1. Introduction

In the last decade it has been shown that the visible spectrum of Classical T Tauri stars (CTTs) is composed of a "normal" stellar spectrum and a smoothly varying continuum with emission lines superposed (Walker 1987; Hartigan et al. 1989, HHKHS hereafter). This continuum excess (excess hereafter) makes the photospheric absorption lines to appear veiled, i.e. less deep than those of a star with the same spectral type. The excess is bluer than the normal stellar continuum and seems to be related with some mechanism of the accretion process: emission from an active photosphere (Calvet et al. 1984), from a boundary layer (Lynden-Bell & Pringle 1974; Bertout et al. 1988), or from the base of magnetospheric accretion columns (Hartmann et al. 1994).

In order to model a CTTs, it is necessary to know the amount of excess, or equivalently, the amount of veiling (defined as the ratio between the excess and the local continuum of the underlying normal star). Several methods have been developped to estimate the veiling. The most popular one is that proposed by HHKHS (see also Basri & Batalha 1990) which consists in comparing, within a small wavelength interval of a few tens of angstroms (where the veiling and the extinction towards the object can be assumed constant), high resolution spectra of a CTTs with a standard star of the same spectral type. More recently, Gullbring et al. (1998, GHCC hereafter) introduced a new method to derive both the visual extinction and the excess spectral shape from spectrophotometrically calibrated data by veiling analysis in a limited number of optimized photospheric absorption lines.

This article intends to study within a rigorous framework, veiling, visual extinction and excess extraction from the spectra of CTTs. Sect. 2 investigates further the method of HHKHS for veiling estimate. We introduce a non linear least square fit which allows to deal with non constant noise, and we derive a formal expression for the resulting error of the veiling. We also discuss the main sources of bias and the influence of the spectral resolution on the veiling estimate. In Sect. 3, we generalize the

method of GHCC for the determination of the visual extinction and excess spectral shape by introducing a "continuous" method which is tested successfully on simulated data. The originality of this new approach is that it uses all the avalaible information contained in the spectra. We derive a formal expression for the visual extinction error and we conclude this work by a brief discussion of the results.

2. Derivation of veiling

In this section, we consider a spectral range small enough for the excess and the extinction to be constant. The reference spectrum S is normalized to its local continuum and the object spectrum O is corrected from any residual continuum slope. In the following for simplicity we do not make the distinction between a parameter and its estimated value and the reference spectrum is assumed to match exactly the underlying object stellar spectrum, unless clearly stated.

2.1. The formalism

In the absence of noise, by definition O and S are related by:

$$O(\lambda)w(\lambda) = p_0\big[S(\lambda) + r\big]w(\lambda), \tag{1}$$

where λ is the wavelength, p_0 a scaling factor, r the veiling, and $w(\lambda)$ a weight which is equal to 0 at unusable wavelength ranges (like emission lines or partially filled lines), and to 1 elsewhere. In the following, we assume that the spectra are sampled at the Shannon frequency at values λ_i for $i = 1, ..., m$, and the entire acquired spectrum is usable, $w(\lambda_i) = 1$. Now we want to estimate the parameters, p_0 and $p_1 = r$. Assuming that the measurement errors are gaussian, the maximum likelihood estimate of the parameters is simply obtained via a least square fit, non linear in this case. To perform the fit, we first define the vector $\mathcal{Q}$, whose components Q_i are:

$$Q_i = \frac{O_i - p_0(S_i + r)}{\sigma_i}, \tag{2}$$

where the index i stands for λ_i, $\sigma_i = (\sigma_{o,i}^2 + p_0^2\sigma_{s,i}^2)^{1/2}$, and $\sigma_{o,i}^2$ and $\sigma_{s,i}^2$ represent the variances of O_i and S_i, respectively. For statistically independent measurements, the correct values of the p's are obtained by minimizing the square modulus of the vector $\mathcal{Q}$ with an iterative procedure, solving at each step the system of equations (see Knoechel & Heide 1978):

$${}^t\mathcal{A}\mathcal{A}\delta\mathcal{P} = {}^t\mathcal{A}\mathcal{Q}, \tag{3}$$

where $\delta\mathcal{P}$ is a vector whose components are δp_0 and $\delta p_1 = \delta r$, i.e. the increment to vector $\mathcal{P}$ whose components are p_0 and $p_1 = r$; ${}^t\mathcal{A}$ is the transpose matrix of the derivatives of $\overline{\mathcal{Q}}$ with respect to the p's, the upper bar over $\mathcal{Q}$ standing for the expected value. The element (i, j) of matrix $\mathcal{A}$ is written as:

$$A_{i,j} = \frac{\partial\overline{Q}_i}{\partial p_j}. \tag{4}$$

For the calculations, $\overline{Q}_i$ can conveniently be approximated by Q_i. At each step, the matrix $\mathcal{A}$ and the vector $\mathcal{Q}$ are then recomputed. The procedure is very robust and it generally converges after a few iterations, if the initial values of the p's are close to the correct ones. At the end of the iterative process, the variance of the p's are the diagonal elements of the matrix $\left[{}^t\mathcal{A}\mathcal{A}\right]^{-1}$. The reduced chi-square value is simply given by ${}^t\mathcal{Q}\mathcal{Q}/(m-2)$ and should be close to 1 for a statistically correct fit.

2.2. Error analysis

The detailed error calculation is given in Appendix A. Generally, the reference star is much brighter than the object source, and its contribution to the noise can be neglected. Indeed, it is important to have a set of good quality reference stars which can be used in any veiling study. Under this assumption, for both photon and constant additive limited noises, within a very good approximation, the standard deviation (error hereafter) of the veiling is given by:

$$\sigma(r) \approx \frac{(1+r)^2}{\epsilon_o {\Delta_{\overline{s}}}^{1/2}}, \tag{5}$$

and the relative error on the scaling factor can be written as:

$$\frac{\sigma(p_0)}{p_0} \approx \frac{1+r}{\epsilon_o {\Delta_{\overline{s}}}^{1/2}}, \tag{6}$$

where ϵ_o is the signal to noise ratio on the object total spectrum flux and $\Delta_{\overline{s}}$ is the variance of the normalized reference spectrum expected value $\overline{S}$. $\Delta_{\overline{s}}$ measures the square of the spectrum contrast and is defined by:

$$\Delta_{\overline{s}} = \frac{\sum_{i=1}^m \overline{S^2}_i}{m} - \left(\frac{\sum_{i=1}^m \overline{S}_i}{m}\right)^2. \tag{7}$$

Clearly, for veiling values greater than 1, the veiling error increases as the square of the veiling which illustrates the difficulty to estimate large veiling values. These results are discussed in Sect. 2.4. The relative veiling error can also be written as:

$$\frac{\sigma(r)}{1+r} \approx \frac{1}{m^{1/2} q_o}. \tag{8}$$

This formula can be useful to estimate rapidly the veiling error from the data and allows us to introduce the contrast spectrum in noise units $q_o = {\Delta_{\overline{o}}}^{1/2}/\sigma_o$ (resp. q_s), which is a central quantity in bias studies.

2.3. Bias problems

There are two main sources of bias in veiling calculation. The first is due to a bad estimate of the noise ratio between the object and the reference. The second is due to mismatches between the object and the reference spectra.

2.3.1. Uncorrect noise estimate

Let us first study the noise problem. We assume for simplicity constant additive noises σ_o for the object and σ_s for the reference. Eq. (2) can then be rewritten as:

$$\sigma_o Q_i = \frac{O_i - p_0(S_i + r)}{(1 + p_0^2\xi_0^2)^{1/2}}, \tag{9}$$

where $\xi_0 = \sigma_s/\sigma_o$. Clearly, Eq. (9) shows that the estimated veiling $r\prime$ depends on the input noise ratio between the reference and the object. If this noise ratio is not correctly estimated, the veiling will be biased. We derive an analytical expression of this bias in Appendix B1. We find that it is a function of the veiling r, q_o and q_s (the contrast of the object and the reference spectra in noise units) and of the quantity $f = \xi/\xi_0$, where $\xi = \sigma\prime_s/\sigma\prime_o$ is the input noise ratio between the reference and the object. The expected value of the estimated veiling $\overline{r\prime}$ lies between two extreme values, $\overline{r\prime}_{max}$ and $\overline{r\prime}_{min}$, which define the range of permitted veiling values compatible with the data, and correspond to $\sigma_i = \sigma\prime_o$ ($f = 0$) and $\sigma_i = p_0\sigma\prime_s$ (f infinite) in Eq. (2), respectively. Defining the extreme relative veiling biasses $\delta r_{max} = \overline{r\prime}_{max} - r$ and $\delta r_{min} = \overline{r\prime}_{min} - r$, it follows that (see Appendix B1):

$$\frac{\delta r_{max}}{\langle\overline{S}\rangle + r} = \frac{1}{q_s^2}, \tag{10}$$

and

$$\frac{\delta r_{min}}{\langle\overline{S}\rangle + r} = -\frac{1}{1+q_o^2}, \tag{11}$$

where the brackets $\langle\rangle$ stand for the mean value. This bias has a very simple explanation. Underestimating the noise ratio ξ_0 is equivalent to underestimate the reference noise σ_s, or equivalently, to overestimate the object noise σ_o. Let us concentrate for example on the reference. If σ_s is underestimated, the algorithm will interpret part of the reference noise in terms of high frequency signal, it will "see" the reference absorption lines apparently deeper than they really are and will tend to overerestimate the object veiling. On the contrary, if σ_s is overestimated, the algorithm will interpret part of the true signal in terms of noise, it will "see" the reference aborption lines less deep than they really are and will then tend to underestimate the object veiling. It is not always easy to estimate the true noise ratio between the reference and the object. But if one of the two sources has a very good signal to noise ratio, usually the reference, then q_s is large and $\overline{r\prime}_{max} \approx r$, as shown in Eq. (10). It is then convenient to set $\sigma_i = \sigma\prime_o$ in Eq. (2): the derived veiling is biased, but the bias is negligible. On the other hand, if q_o is large, $\overline{r\prime}_{min} \approx r$ [see Eq. (11)]: in this case it is better to set $\sigma_i = p_0\sigma\prime_s$ in Eq. (2). If both q_s and q_o are small, the bias can be very important even if the input noise ratio is not correct by only a factor of 2 (as shown in Figs. B1a and B1b). In case of doubt, one can minimize the bias by underestimating or overestimating the noise ratio ξ_0, depending if q_s is larger or smaller than q_o, respectively.

To conclude this section, we generally recommend to filter the spectra before veiling calculation, but the choice of the working spectral resolution must be examined case by case. The spectra between 5180 Å and 5220 Å presented in Fig. 1 of Hartmann & Kenyon (1990) are typical examples. Indeed, we can see the presence of high frequency noise superposed on lower frequency structures. Filtering these data by a factor of a few will considerably reduce the noise without affecting significantly the spectrum contrast, which in turn will greatly decrease the possible bias due to a bad noise estimate at a negligible cost in terms of the veiling error.

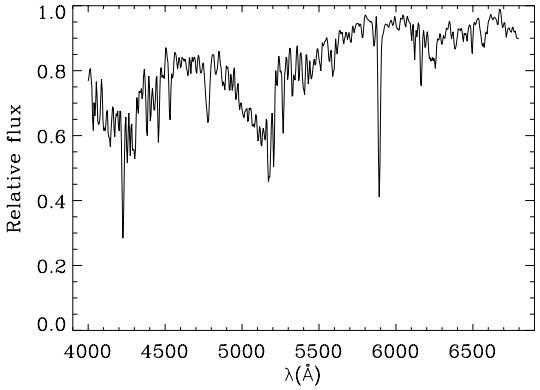

Fig. 1. Spectrum of the K7V star HD 201092, first normalized to its local continuum at $R = 40000$ and filtered at $R = 500$.

2.3.2. Mismatches between the object and the reference spectra

The other source of bias, regards mismatches between the object and the reference spectra, and it is treated in details in Appendix B2. By mismatches, we mean spectral differences between the reference spectrum and the true underlying object stellar spectrum T and/or systematic errors of any kind. We show that if the contrast of the object and the reference spectra are large compared to the residual of the veiling equation, then the bias is dominated by the apparent veiling r_s of S with respect to T. Defining the bias by $\delta r = r_c - r$, where r_c is the calculated veiling, the relative bias is written:

$$\frac{\delta r}{\langle\overline{S}\rangle + r} = -r_s. \tag{12}$$

In the case of non noisy data, the validity of Eq. (12) can be checked by computing the extreme veiling values r_M and r_m obtained from $\xi = 0$ and ξ infinite, respectively. If these two values coincide, then Eq. (12) is correct. Otherwise, we must add to Eq. (12) another bias which depends on the input ξ value. The distance between r_M and r_m is a good indicator to evaluate the importance of mismatches between S and T, which cannot be interpreted in terms of veiling. It also probably gives a good order of magnitude of the resulting bias.

2.4. The effect of the spectral resolution

In this section, we study the effect of the spectral resolution on the veiling value and the associated noise. For this purpose, we use a high quality spectrum of the K7V star HD 201092, obtained at the 1.93m telescope of the Observatoire de Haute Provence (France) with the instrument ELODIE, at $R = 40000$ (see Baranne et al. 1995) and for which $\overline{S} \approx S$ and $\Delta_{\overline{s}}^{1/2} \approx \Delta_s^{1/2}$. Fig. 1 shows this spectrum between 4000 Å and 6800 Å, normalized to its local continuum at $R = 40000$ and then filtered at $R = 500$.

Defining as we did so far, the veiling as the ratio between the excess and the local stellar continuum, does not provide an absolute quantity, because the level of the local continuum is resolution dependent. To study the effect of the spectral reso-

lution on the veiling value, we have selected a spectral band of 40 Å centered at 5200 Å from our K7V star, normalized to its local continuum to simulate the reference, and added a veiling of 1 to the reference to simulate the object. We then degrade the spectral resolution of both the object and the reference by gaussian filtering, and estimate the veiling, renormalizing first the reference spectrum to its new local continuum. The veiling is found to vary by about 10% when the spectral resolution varies from 40000 to 500. However, the product of the veiling with the spectrophotometrically calibrated local continuum of the reference spectrum, which measures the excess, will obviously remain unchanged. Defining the veiling as the ratio between the excess and the mean reference flux (see HHKHS) would result in a quantity little dependent on the spectral resolution.

The veiling error, Eq. (5), is inversely proportional the product $\epsilon_0 \Delta_s^{1/2}$ which is sensitive to the spectral resolution R. Fig. 2 shows $\Delta_s^{1/2}$ between 4000 Å and 6600 Å, computed from our K7V spectrum for various spectral resolutions, every 50 Å in a wavelength interval of 100 Å. It has two maxima, the first around 4300 Å and the second, slightly higher around 5200 Å. This explains why veiling studies are often performed around 5200 Å. Indeed, this wavelength combines a high spectrum contrast $\Delta_s^{1/2}$ with a good experimental response. However, the region around 4300 Å can also be interesting if the signal to noise ratio is high enough. At most wavelengths $\Delta_s^{1/2}$ varies *only* by a factor of 2 to 4 from $R = 500$ to $R = 40000$. For a given integration time and wavelength interval, the signal to noise ratio on the object total spectrum flux ϵ_o is obviously independent on R for photon and background limited noises. However, for CCD readout limited noise, it is inversely proportional to the square root of the number of pixels, i.e. the square root of R. Hence, if we take only into account the statistical noise, we conclude that within a factor of a few, the veiling error is independent on the spectral resolution and can even increase with the latter for readout limited noise. However in practice, it will be difficult to estimate the veiling in a 100 Å interval at spectral resolutions as low as a few hundreds. A first reason is that, excluding the unusable features, the useful spectrum could be reduced to only a few points, leading to a high veiling error. More important, at such low spectral resolutions the spectrum contrast is generally small (of the order of a few%) and can become comparable to systematic local errors (probably of the order of one to a few %) leading to important biasses. For moderatly veiled T Tauri stars, these difficulties can be overcome by working on large structures of high contrast like the one extending from 4900 Å to 5250 Å in Fig. 1 ($\Delta_s^{1/2} \approx 0.1$). Although on such a large spectral bandwidth, the formalism of Sect. 2.1 cannot be applied, the problem can be solved by simple polynomial model fitting (Chelli et al. 1997; Chelli, in preparation).

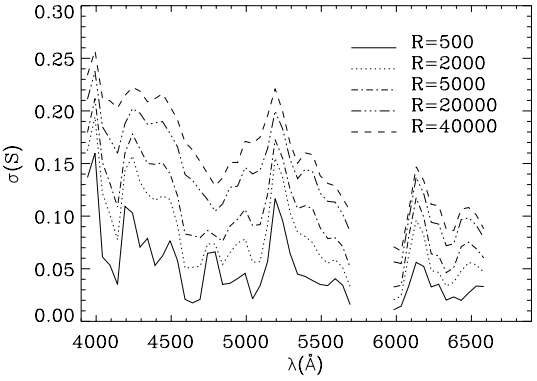

Fig. 2. Variance, for various spectral resolutions, of a K7V reference spectrum normalized to its continuum and computed every 50 Å over a 100 Å bandwidth. The strong Na doublet in absorption around 5893 Å, often partially filled in CTTs, has been excluded from the calculation.

3. Derivation of visual extinction and excess spectral shape

In the last decade, it has been realized that because of the excess, the visual extinction could not be deduced directly from the colors of T Tauri stars. Hartigan et al. (1991) proposed to estimate the extinction towards T Tauri stars, combining colors and veiling measurements in the V band. Recently, GHCC extended the previous method by the use of spectrophotometry and veiling analysis of a few photospheric absorption lines spanned over a large spectral bandwidth. Then, combining the extinction and the calibrated spectra, they were able to deduce the excess spectral distribution. We propose here to generalize the discrete method of GHCC by a "continous" approach which uses *all* the information contained in the spectra.

In this section, the whole spectrum of our K7V star between 4000 Å and 6800 Å, except the deep Na doublet around 5893 Å, is used as the reference spectrum. As the former was first normalized to its local continuum, the excess and the veiling are represented, without any loss of generality, by the same quantity.

3.1. The formalism

We assume that the object and the reference spectra, $O(\lambda)$ and $S(\lambda)$, are observed at a spectral resolution R, are already calibrated spectrophotometrically, and that the reference spectrum has been corrected for extinction. In the absence of noise, $O(\lambda)$ and $S(\lambda)$ are strictly related by the following equation (see GHCC):

$$O(\lambda)w(\lambda) = p_0 10^{-0.4 f(\lambda) A_v} \big[S(\lambda) + E(\lambda)\big] w(\lambda), \qquad (13)$$

where A_v is the visual extinction towards the object, $f(\lambda) = A_\lambda / A_v$ describes the extinction law, and $E(\lambda)$ is the continuum excess flux (the other quantities are defined in Sect. 2.1).

It is useful to first examine the approach of GHCC. Let $n\prime$ be the number of fit photospheric lines at the wavelengths λ_k, $k = 1, ..., n\prime$. The output of their discrete method consists in a set of local scaling factors $\{p_{0,k}\}$ and excesses $\{E_k\}$. In the absence of noise, each $p_{0,k}$ is related to A_v and to the overall scaling factor p_0 by:

$$p_{0,k} = p_0 10^{-0.4 f_k A_v}. \qquad (14)$$

In practice, A_v and p_0 are obtained by minimizing a set of $n\prime$ relations via Eq. (14), which in turn, allows to derive the excess by inverting Eq. (13):

$$E(\lambda) = \frac{10^{0.4f(\lambda)A_v}}{p_0}O(\lambda) - S(\lambda). \quad (15)$$

The method of GHCC is very interesting and its basic idea is innovating. However, because of its discrete nature, it discards an important part, perhaps most, of the information contained in the spectra, in particular their low frequency structure. In the general case, it is not possible to solve directly Eq. (13) because we do not know the functional dependence of $E(\lambda)$. However, what we know is that it is a smooth function of the wavelength and this information can conveniently be used in a "continuous" modelling.

Let us now introduce our approach. In a given spectral interval $\Delta\lambda$, any well-behaving physical function like the excess can be decomposed into the sum of a straight line joining its end points and the Fourier series of a periodical function over $\Delta\lambda$. The excess being smooth, the Fourier series can be truncated at a certain maximum order n. Under these conditions, $E(\lambda)$ can be expressed in the form:

$$E(\lambda) = a\lambda + \sum_{j=0}^{n} b_j cos\Big(2\pi j\frac{\lambda}{\Delta\lambda}\Big) + \sum_{j=1}^{n} c_j sin\Big(2\pi j\frac{\lambda}{\Delta\lambda}\Big). \quad (16)$$

The problem reduces to the estimate of the $2n+4$ parameters $(p_0, A_v, a, \{b\}, \{c\})$, with $\{b\} = (b_0, ..., b_n)$ and $\{c\} = (c_1, ..., c_n)$, but the formalism of Sect. 2.1 can be generalized to any number of parameters. Assuming that the wavelength is sampled at the Shannon frequency at values λ_i and that $w(\lambda_i) = 1$ (for $i = 1, ..., m$), we define the vector $\mathcal{Q}$, of components Q_i, whose square modulus is to be minimized, with:

$$Q_i = \frac{O_i - p_0 10^{-0.4 f_i A_v}\left[S_i + E_i(a, \{b\}, \{c\})\right]}{\left(\sigma_{o,i}^2 + p_0^2 10^{-0.8 f_i A_v}\sigma_{s,i}^2\right)^{1/2}}, \quad (17)$$

and:

$$E_i(a, \{b\}, \{c\}) = ai + \sum_{j=0}^{n} b_j cos\Big(2\pi j\frac{i}{m}\Big) + \sum_{j=1}^{n} c_j sin\Big(2\pi j\frac{i}{m}\Big). \quad (18)$$

The excess cut-off frequency is controlled by the parameter n and the associated spectral resolution R_e is simply given by:

$$R_e = \frac{2n}{m}R. \quad (19)$$

If R_e is smaller than R, then $2n < m$, our problem is well defined and the solution of the fit is unique. The excesses determined by GHCC on 17 T Tauri stars show that this is in practice always the case. Indeed, they vary very smoothly with a cut-off frequency smaller than a few tens, which corresponds to $R_e/R \lesssim 0.1$, even at spectral resolutions as low as a few hundreds.

3.2. How does it work?

To understand how the algorithm works, let us go back to the discrete approach of GHCC. A_v and p_0 are derived from a least square fit of the set of local scaling factors $\{p_{0,k}\}$. Assuming as in Sect. 2 that the noise on the reference spectrum is negligible, the error on each $p_{0,k}$, given by Eq. (6), is inversely proportional the the spectrum contrast. For constant veiling and signal to noise ratio ϵ_0, the procedure will weight more the regions of high contrast with respect to the regions of low contrast which, incidentally, are also more sensitive to biasses. Now, if instead of fitting individual lines, we use the whole spectrum divided into equal intervals where the extinction and the excess can be considered constant, the same analysis applies. By extrapolation, the same argument is valid for our "continuous" approach, which can be considered as the limit when the length of each interval tends to zero. As we do not know *a priori* the excess cut-off frequency, we have to vary the parameter n increasing it and computing at each spectral resolution the outputs of the fit, until the visual extinction and the overall scaling factor stabilize within the error bars. This will happen when the true excess cut-off frequency is reached.

In order to test the algorithm, we have performed a number of simulations at low spectral resolution ($R = 500$) with the reference spectrum of Fig. 1. The object spectra were generated by combining the reference spectrum with a large number of "smooth" excess (or veiling) shapes, visual extinction values, and white noise. R_e was varied from small values to 150. We find that in all cases, the computed visual extinction and overall scaling factor stabilizes around the correct ones, within the error bars, after a critical spectral resolution has been reached (which depends on the excess cut-off frequency). The best estimates of the parameters correspond to those where the errors are the smallest., i.e. when the parameters begin to stabilize. Figs. 3 and 4 show two examples of simulations. The extreme excess shape of Fig. 3a (solid line) was generated from a random function of unit mean and variance, smoothed by gaussian filtering at a spectral resolution of 50. The associated object spectrum of Fig. 3b exhibits a visual extinction of 2 and an average signal to noise ratio of 100. We see in Figs. 3c and 3d that the computed A_v begins to stabilize to the correct value and that the reduced chi-square value ${}^t\mathcal{Q}\mathcal{Q}/(m-2n-4)$ reaches 1 and remains constant, at about $R_e/R = 0.1$ or, equivalently, at $R_e = 50$. The optimum visual extinction value, taken at the beginning of the plateau, is $A_v = 2.08 \pm 0.10$. The corresponding excess, deduced from Eq. (15) (dotted line in Fig. 3a) shows a quasi perfect agreement with that in input. Fig. 4a represents a more realistic excess (solid line) of unit mean value generated by summing up a constant and an exponential function. The associated object of Fig. 4b exhibits a visual extinction of 1 and an average signal to noise ratio of 50. Here, the computed A_v begins to stabilize at $R_e/R = 0.05$ or $R_e = 25$, for which $A_v = 1.01 \pm 0.15$. The spectral shape of the corresponding excess (dotted line in Fig. 4a) shows an excellent agreement with that in input, only 10% smaller. The reduced chi-square value of Fig. 4d varies from 0.94 to 0.90, clearly showing that the goodness of the fit

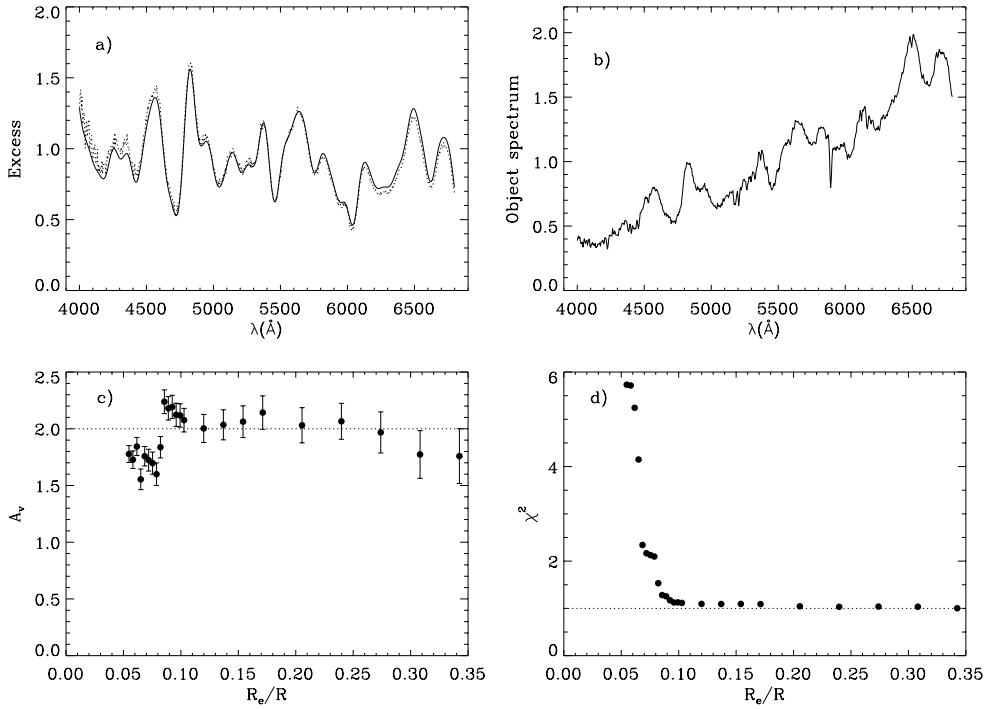

Fig. 3. a *Solid line:* model of the excess; *dotted line:* reconstructed excess at $R_e = 50$. **b** Object spectrum generated from the excess model and the reference spectrum at a spectral resolution $R = 500$; the input visual extinction is $A_v = 2$ and the average signal to noise ratio $\langle N \rangle$ is 100. **c** Calculated visual extinction as a function of R_e/R, A_v begin to stabilize, within the noise, at the correct value, from $R_e/R = 0.1$ or $R_e = 50$. **d** Reduced chi-square as a function of R_e/R.

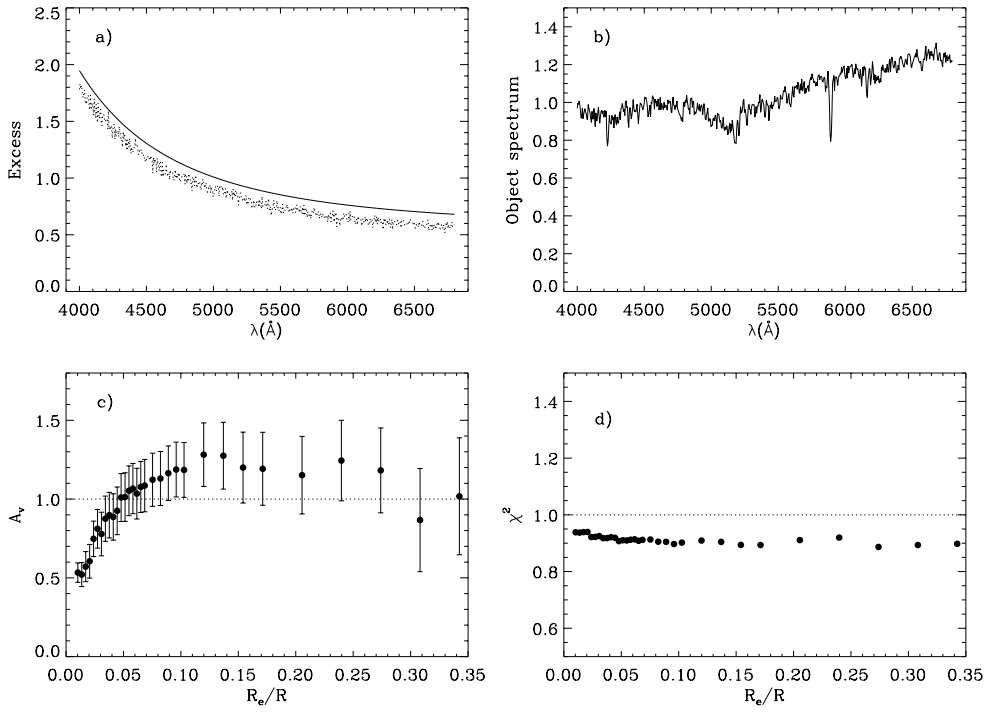

Fig. 4. a *Solid line:* model of the excess; *dotted line:* reconstructed excess at $R_e = 25$. **b** Object spectrum generated from the excess model and the reference spectrum at a spectral resolution $R = 500$; the input visual extinction is $A_v = 1$ and the average signal to noise ratio $\langle N \rangle$ is 50. **c** Calculated visual extinction as a function of R_e/R, A_v begin to stabilize, within the noise, at the correct value, from $R_e/R = 0.05$ or $R_e = 25$. **d** Reduced chi-square as a function of R_e/R (see text).

has not to be judged on the basis of the reduced chi-square value, but on the existence of a plateau in which the computed visual extinction remains, within the noise, constant as a function of R_e.

3.3. Error analysis

In this section we derive a formal expression for the errors on the visual extinction and the overall scaling factor. A careful

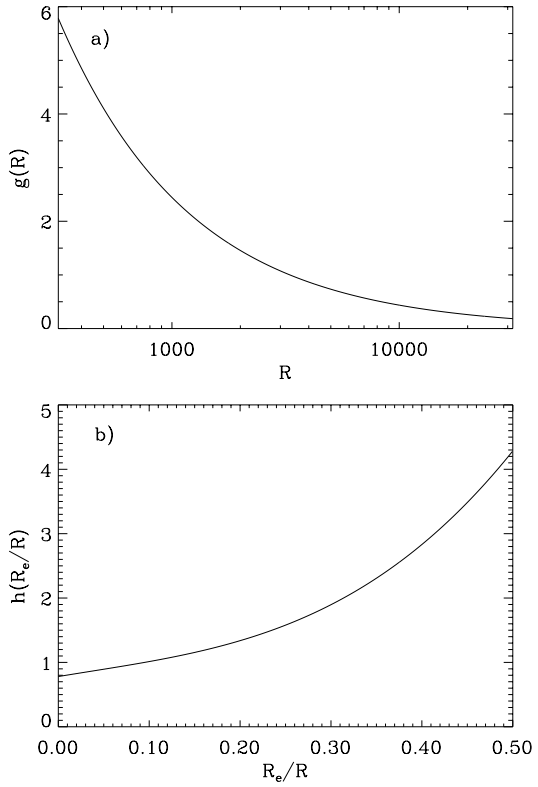

Fig. 5. a $g(R)$ as a function of the spectral resolution R, **b** $h(R_e/R)$. The error on the visual extinction is proportional to the product of these two functions (see text).

examination of the matrix $[{}^t\mathcal{A}\mathcal{A}]^{-1}$ associated to the discrete case shows that:

$$\frac{\sigma(p_0)}{p_0} \approx \sigma(A_v), \tag{20}$$

and that within a good approximation:

$$\sigma(A_v) \propto \frac{1+\langle r\rangle}{\langle N\rangle}, \tag{21}$$

where $\langle r\rangle$ and $\langle N\rangle$ represent the average veiling and the average signal to noise ratio on the object spectrum, respectively.

Eqs. (20) and (21) are also valid in the limit of our "continuous" approach. To evaluate the coefficient of proportionality in Eq. (21), we performed a number of simulations with our reference spectrum. The object spectra were generated by adding a constant veiling to the reference and introducing various visual extinctions. The spectral resolutions, R and R_e, were controlled by filtering and by varying the number of parameters n, respectively. Numerical calculations of the diagonal elements of the corresponding matrix $[{}^t\mathcal{A}\mathcal{A}]^{-1}$ show that the coefficient of proportionality is, in a first approximation, independent on the visual extinction. It increases by only a factor of two when increasing the extinction from 0 to 5, and can be well approximated by the product of two functions, $g(R)$ and $h(R_e/R)$. Hence, the error on the visual extinction can be written as:

$$\sigma(A_v) \approx g(R)h(R_e/R)\frac{1+\langle r\rangle}{\langle N\rangle} \tag{22}$$

Figs. 5a and 5b show the functions $g(R)$ and $h(R_e/R)$. As expected, $g(R)$ is a decreasing function of R whereas $h(R_e/R)$ is an increasing function of R_e/R approximatively equal to 1 for $R_e/R \lesssim 0.1$. The visual extinction error is basically controlled by the function $g(R)$, which depends only on the input reference spectrum. Comparison of Eqs. (6), (20) and (22) shows that the higher the reference spectrum contrast, the smaller the function $g(R)$. Hence, we can easily infer that for M stars, whose spectra are generally more contrasted that those of K stars, the corresponding $g(R)$ function is smaller than that shown in Fig. 5a. On the other hand, it will be larger for G stars or earlier spectral types. GHCC pointed out that to work their method needed absorption lines spanning over a large spectral bandwidth. As well, in our "continuous" approach, we need different regions of high contrast, otherwise the function $g(R)$ would be prohibitively large. Therefore, it is illusory trying to estimate any visual extinction from a spectrum by using only one absorption line and an arbitrary amount of continuum.

3.4. Discussion and conclusions

A specific problem of the "continuous" approach could be the use of large spectral bandwidths because of wavelength calibration errors. For example, mismatches of spectral lines between the object and the reference may introduce spurious high frequency noise in the calculated excess. The smooth excesses derived by GHCC in a bandwidth larger than 1000 Angstroms show that, at least here, this does not seem to be a severe limitation (see in particular the case of DS Tau). Also, it may occur that the calculated visual extinction never stabilizes when increasing the veiling spectral resolution. For a statistically correct fit, the absence of convergence means that either the template is not adequate or the object has a complex spectrum which cannot be fit by a simple extinction and excess model.

Eq. (22) can be used to study the variation of the visual extinction error as a function of the spectral resolution. Assuming photon or background limited noise, for a given integration time $\langle N\rangle$ is inversely proportional to the square root of R. The error $\sigma(A_v)$ is represented in Fig. 6 as a function of R, for zero veiling and visual extinction, $R_e = 50$ and $\langle N\rangle = 100$ at $R = 500$. It is practically proportional to $g(R)R^{1/2}$ and decreases from 0.04 at $R = 500$, by about a factor of 2 at $R = 2000$, and a further factor of 4 going to $R = 30000$. Taking only into account the statistical noise, there is not much gain at high spectral resolution when using the whole spectrum in the "continuous" approach proposed here. Moreover, the factor 4 quoted above is indeed an upper limit, because in reality higher resolutions correspond to smaller optical transmission due to the more sophisticated experimental set-up. The error given in Eq. (22) represents, however, what we can hope for in the absence of systematic errors. In practice, at high spectral resolution the contrast of the spectra is higher, and consequently the output parameters are less sensitive to biasses than at low spectral resolution. It is also easier to identify emission lines and local spectral mismatches, and hence, the usable spectral bandwidth is larger. Therefore, it will probably be dif-

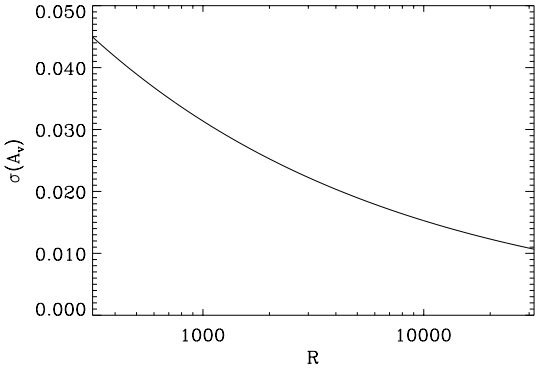

Fig. 6. Error on the estimated visual extinction for a given integration time, for zero veiling and visual extinction, derived from the spectrum of a K7V star between 4000 Å and 6800 Å, as a function of the spectral resolution R. The excess spectral resolution is $R_e = 50$ and the average signal to noise ratio on the object spectrum is $\langle N \rangle = 100$ at the spectral resolution $R = 500$. The dominant source of error was assumed to be photon or background noise.

ficult to handle resolutions of a few hundreds, for highly veiled T Tauri stars or when the excess is dominated by emission lines.

The statistical error given in Eq. (22) is much smaller than the experimental errors estimated by GHCC who pointed out that they are limited by systematic errors. Hence, if the systematic errors are not coupled to the statistical noise, we conclude that it is in principle possible to study objects much fainter than those so far studied by using the "continuous" approach over a large spectral bandwidth. This conclusion is further reinforced by the fact that there is no need to correctly isolate some individual photospheric absorption lines for veiling calculation, as it is the case with the discrete method. This is an important advantage which can greatly help to work on noisy spectra. There are some remaining questions about our "continuous" approach: What is the best spectral resolution? What is the sensitivity to systematic errors? What are the performances of the proposed method with respect to others? All these questions have to be adressed experimentally.

Appendix A: veiling error

From Eq. (2) and (4), we can easily compute the matrix $\mathcal{A}$ and then the matrix $\left[{}^t\mathcal{A}\mathcal{A}\right]^{-1}$. The veiling variance $\sigma^2(r)$ is written:

$$\sigma^2(r) = \frac{1}{p_0^2} \frac{\sum_{i=1}^m (\frac{\overline{S}_i + r}{\sigma_i})^2}{\sum_{i=1}^m (\frac{\overline{S}_i + r}{\sigma_i})^2 \sum_{i=1}^m \frac{1}{\sigma_i^2} - (\sum_{i=1}^m \frac{\overline{S}_i + r}{\sigma_i^2})^2}, \quad \text{(A1)}$$

and that on the scaling factor is given by:

$$\sigma^2(p_0) = p_0^2 \sigma^2(r) \frac{\sum_{i=1}^m \frac{1}{\sigma_i^2}}{\sum_{i=1}^m (\frac{\overline{S}_i + r}{\sigma_i})^2}, \quad \text{(A2)}$$

where the upper bar over S_i stands for the expected value, r is the veiling of the object and $\sigma_i = (\sigma_{o,i}^2 + p_0^2 \sigma_{s,i}^2)^{1/2}$, where $\sigma_{o,i}^2$ and $\sigma_{s,i}^2$ represent the variances of O_i and S_i, respectively.

Making the approximation $S_i + r \approx 1 + r$, the relative error on the scaling factor is written:

$$\frac{\sigma(p_0)}{p_0} = \frac{\sigma(r)}{1 + r}. \quad \text{(A3)}$$

The value of p_0 is simply obtained by applying Eq. (2) to the continua:

$$p_0 = \frac{\overline{O}_c}{1 + r}, \quad \text{(A4)}$$

where $\overline{O}_c$ is the expected value of the object continuum. In the following, we assume, for simplicity and whithout loss of generality, that the noise of the reference spectrum is much smaller than that of the object spectrum and can be neglected, $\sigma_i \approx \sigma_{o,i}$. Now we consider constant additive and photon limited noises.

A.1. Constant additive noise

Setting $\sigma_i = \sigma_o$, inserting Eq. (A4) into Eq. (A1) and using the relation:

$$\frac{\overline{O}_i}{\overline{O}_c} = \frac{\overline{S}_i + r}{1 + r}, \quad \text{(A5)}$$

it comes after some transformations:

$$\sigma(r) = a_1 \frac{(1 + r)^2}{\epsilon_o \Delta_{\overline{s}}{}^{1/2}}. \quad \text{(A6)}$$

$\Delta_{\overline{s}}$ is the variance of the reference spectrum expected value $\overline{S}$, given by:

$$\Delta_{\overline{s}} = \frac{\sum_{i=1}^m \overline{S^2}_i}{m} - \left(\frac{\sum_{i=1}^m \overline{S}_i}{m} \right)^2, \quad \text{(A7)}$$

$\epsilon_0 = m^{1/2} \langle \overline{O} \rangle / \sigma_o$ is the signal to noise ratio on the object total spectrum flux, $\langle \overline{O} \rangle = \frac{1}{m} \sum_{i=1}^m \overline{O}_i$ and a_1 is written:

$$a_1 = \frac{1}{m} \sum_{i=1}^m \frac{\overline{S}_i + r}{1 + r} \times \left(\frac{1}{m} \sum_{i=1}^m \left(\frac{\overline{S}_i + r}{1 + r} \right)^2 \right)^{1/2}. \quad \text{(A8)}$$

A rapid examination of Eq. (A8) shows that the coefficient a_1 is always close to 1.

A.2. Photon limited noise

Here, $\sigma_i = O_i{}^{1/2}$. Inserting Eqs. (A4) into Eq. (A1) and using Eq. (A5), it comes:

$$\sigma(r) = a_2 \frac{(1 + r)^2}{\epsilon_o \Delta_{\overline{s}}{}^{1/2}}, \quad \text{(A9)}$$

where $\epsilon_0 = m^{1/2} \langle \overline{O} \rangle^{1/2}$ is the signal to noise ratio on the object total spectrum flux and a_2 is given by:

$$a_2 = \frac{\Delta_{\overline{s}}^{1/2}}{1 + r} \frac{1}{m} \sum_{i=1}^m \frac{\overline{S} + r}{1 + r} \times \left(\frac{1}{m} \sum_{i=1}^m (\overline{S}_i + r) \frac{1}{m} \sum_{i=1}^m \frac{1}{\overline{S}_i + r} - 1 \right)^{-1/2}. \quad \text{(A10)}$$

Numerical calculations using our K7V spectrum show that the coefficient a_2 is generally close to 1 for any veiling value.

Note that using the relation $\Delta_{\overline{o}}^{1/2} \approx \langle\overline{O}\rangle\Delta_{\overline{s}}^{1/2}/(1+r)$, the relative veiling error for additive and photon noise takes the very simple form:

$$\frac{\sigma(r)}{1+r} \approx \frac{1}{m^{1/2}q_o}, \tag{A11}$$

where $q_o = \Delta_{\overline{o}}^{1/2}/\sigma_o$ is the contrast of the object spectrum in noise units.

Appendix B: bias calculation

B.1. Uncorrect noise estimate

We assume constant additive noises σ_o for the object and σ_s for the reference. Under these conditions, the estimated veiling value $r\prime$ has the following analytical expression (see HHKHS):

$$r\prime = \frac{\langle O\rangle}{C} - \langle S\rangle, \tag{B1}$$

with:

$$C = \frac{-\Delta_s + \xi^2\Delta_o + (\Delta_s^2 - 2\xi^2\Delta_o\Delta_s + \xi^4\Delta_o^2 + 4\xi^2\Delta_{so}^2)^{1/2}}{2\xi^2\Delta_{so}}. \tag{B2}$$

$\langle O\rangle$ and Δ_o (resp. $\langle S\rangle$ and Δ_s) are defined in Appendix A, $\Delta_{so} = \frac{1}{m}\sum O_iS_i - \frac{1}{m^2}\sum O_i\sum S_i$ and ξ is the input noise ratio $\sigma\prime_s/\sigma\prime_o$ between the reference and the object. The expressions $\langle\rangle$ and Δ are yet averaged quantities over the number of points m and so, are close to their expected values. For example, $|\langle O\rangle - \langle\overline{O}\rangle| \approx \sigma_o/m^{1/2}$ and $|\Delta_o - \overline{\Delta_o}| \approx \sigma_o^2/m^{1/2}$. Hence, a good approximate of the expected value $\overline{r\prime}$ of $r\prime$ can be obtained by taking the expected value of the series development to the second order of $r\prime$ around the expected values of the $\langle\rangle$'s and the Δ's (see Papoulis 1965). We find that, within a relative precision of $\frac{1}{m}$, $\overline{r\prime}$ is given by:

$$\overline{r\prime} = \frac{\langle\overline{O}\rangle}{C\prime} - \langle\overline{S}\rangle, \tag{B3}$$

where $C\prime$ is derived from C by replacing the Δ's by their expected values. Let r be the correct veiling, we define the bias by $\delta r = \overline{r\prime} - r$. From Eq. (B3), using the relations $\overline{\Delta_o} = \Delta_{\overline{o}} + \sigma_o^2$, $\overline{\Delta_s} = \Delta_{\overline{s}} + \sigma_s^2$ and $\overline{\Delta_{so}} = \Delta_{\overline{so}}$, and after some simple transformations, the relative bias $\delta r/(\langle\overline{S}\rangle + r)$ is written:

$$\frac{\delta r}{\langle\overline{S}\rangle + r} \approx \frac{1}{\frac{1}{2}\left(1 + \frac{f^2-1-q_s^2}{q_o^2f^2}\right) + \left(\frac{1}{4}\left(1 + \frac{f^2-1-q_s^2}{q_o^2f^2}\right)^2 + \frac{q_s^2}{q_o^2f^2}\right)^{1/2}} - 1, \tag{B4}$$

where q_o (resp. q_s) is defined in Appendix A, and $f = \xi/\xi_0$, with $\xi_0 = \sigma_s/\sigma_o$. It can be verified that for $f = 1$, there is no bias, i.e. $\delta r = 0$. We also checked the general validity of Eq. (B4) through simulations, using the spectrum S of Sect. 2.4 with R=40000, centered at 5200 Å and of width 40 Å.

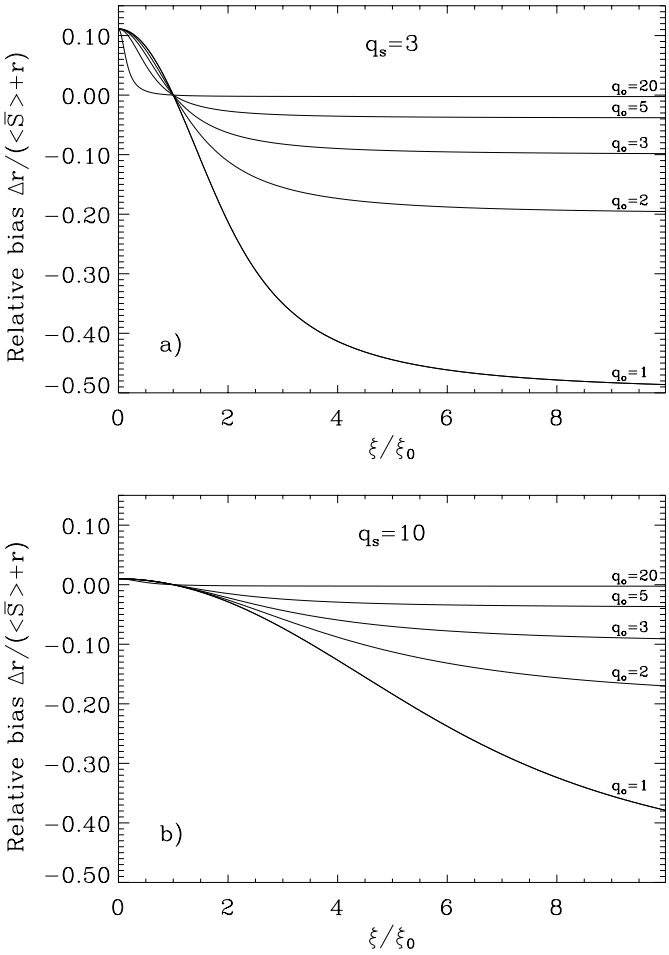

Fig. B1a and b. Relative bias on the estimated veiling as a function of the input error ratio between the reference and the object, normalized to the true error ratio, ξ/ξ_0: **a** for $q_s = \Delta_s^{1/2}/\sigma_s = 3$ and various values of $q_o = \Delta_o^{1/2}/\sigma_o$, **b** for $q_s = 10$.

Two limiting cases are particularly interesting. The first one, $f = 0$, assumes that the noise associated with the reference is zero, $\sigma_i = \sigma\prime_o$ in Eq. (2). The derived veiling expected value $\overline{r\prime}_{max}$ is maximum, the relative bias is positive and is given by:

$$\frac{\delta r_{max}}{\langle\overline{S}\rangle + r} = \frac{1}{q_s^2}. \tag{B5}$$

The second case corresponds to f infinite, it assumes that the noise associated with the object is zero, $\sigma_i = p_0\sigma\prime_s$ in Eq. (2). The derived veiling expected value $\overline{r\prime}_{min}$ is minimum, the relative bias is negative and is given by:

$$\frac{\delta r_{min}}{\langle\overline{S}\rangle + r} = -\frac{1}{1+q_o^2}. \tag{B6}$$

Figs. B1a and B1b show the relative bias as a function of f for various values of q_s and q_o.

B.2. Mismatches between the object and the reference spectra

We assume here that the measured object and reference spectra O and S are not noisy, i.e. $\sigma_s = \sigma_o = 0$, and for simplicity that the object spectrum is unbiased. Let us study for example the problem of mismatches between the reference spectrum S and the underlying object stellar spectrum T. In the absence of systematic errors, we define r_s as the apparent veiling of the reference with respect to T (calculated for example for the limit $\xi = 0$) and γ_1 the residual function of the veiling equation. S can be written as follows:

$$S = \frac{T + r_s}{1 + r_s} + \gamma, \tag{B7}$$

with $\gamma = \gamma_1 + \gamma_2$, where γ_2 represents the systematic error function. If S is an exact veiled version of T, i.e. $\gamma = 0$, then the object veiling with respect to S must be independent of any input noise ratio ξ. Let us examine the extreme object veiling values r_M and r_m obtained for the limits $\xi = 0$ and ξ infinite, respectively. From Eq. (B1) and (B2), r_M and r_m have very simple analytical expressions:

$$r_M = \frac{\Delta_s}{\Delta_{so}}\langle O\rangle - \langle S\rangle, \tag{B8}$$

and

$$r_m = \frac{\Delta_{so}}{\Delta_o}\langle O\rangle - \langle S\rangle. \tag{B9}$$

Let r be the correct object veiling with respect to T, obtained for example by replacing S by T in Eq. (B8). We define the biasses δr_M and δr_m by $\delta r_M = r_M - r$ and $\delta r_m = r_m - r$. Combining Eqs. (B7), (B8) and (B9) and after some transformations, the relative veiling biasses are written:

$$\begin{aligned}\frac{\delta r_M}{\langle T\rangle + r} &= -\frac{r_s}{1 + r_s}\left(\frac{1 + r}{\langle T\rangle + r}\right) - \frac{\langle\gamma\rangle}{\langle T\rangle + r} \\ &\quad + \frac{\Delta_{\gamma T} + (1 + r_s)\Delta_\gamma}{\Delta_T + (1 + r_s)\Delta_{\gamma T}},\end{aligned} \tag{B10}$$

and

$$\frac{\delta r_m}{\langle T\rangle + r} = -\frac{r_s}{1 + r_s}\left(\frac{1 + r}{\langle T\rangle + r}\right) - \frac{\langle\gamma\rangle}{\langle T\rangle + r} + \frac{\Delta_{\gamma T}}{\Delta_T}. \tag{B11}$$

They are the sum of three terms and differ only through the third term. The first term is due to the apparent veiling of the reference S with respect to T. Assuming $1 + r_s \approx 1$ and $\langle T\rangle + r \approx 1 + r$, it can be approximated by $-r_s$. The second and the third terms are due to real spectral mismatches and to systematic errors. The second term is in general negligible, because we expect the mean value of γ to be close to zero for local mismatches of the order of a few% only. The third term is scaled by the ratios $\Delta_{\gamma T}/\Delta_T$ and Δ_γ/Δ_T and is also negligible if the spectrum contrast $\Delta_T^{1/2}$ is large compared to the residual function γ. Under these conditions, the bias due to mismatches between the object and the reference is dominated by the apparent veiling of the reference. Setting $\delta r = \delta r_M = \delta r_m$ and making the approximation $\langle T\rangle \approx \langle S\rangle$, the relative bias is simply given by:

$$\frac{\delta r}{\langle S\rangle + r} = -r_s. \tag{B12}$$

To investigate further the third term in Eqs. (B10) and (B11), it is interesting to calculate the relative difference between r_M and r_m. It is given by:

$$\frac{r_M - r_m}{\langle T\rangle + r} = (1 + r_s)\frac{\Delta_\gamma}{\Delta_T}\left(\frac{1 - \Gamma_{\gamma T}^2}{1 + (1 + r_s)\frac{\delta_{\gamma T}}{\Delta_T}}\right), \tag{B13}$$

where $\Gamma_{\gamma T}$ is the correlation coefficient between γ and T. Eq. (B13) clearly shows that the two veiling values r_M and r_m are equal only if the γ is the null function or if it is a linear function of T. As the latter possibility is unlikely, the equality between r_M and r_m implies necessarily that the γ function is null and consequently that Eq. (B12) is valid. On the other hand, if r_M and r_m are distinct, the third term in Eqs. (B10) and (B11) cannot either be neglected. It introduces another additive bias which depends on the input ξ value. The distance between r_M and r_m is a good indicator to evaluate the importance of mismatches between S and T which cannot be interpreted in terms of veiling, and probably gives also a good order of magnitude of the resulting bias.

Acknowledgements. The author would like to thank the referee Dr. P. Hartigan for his helpful comments that improved the clarity of the paper and Dr. C. Ceccarelli for her careful english revision of the paper and helpful discussions.

References

Baranne A., Queloz Q., Mayor M., et al., 1995, A&AS 119, 373
Basri G., Batalha C., 1990, ApJ 363, 654
Bertout C., Basri G., Bouvier J., 1988, ApJ 330, 350
Calvet N., Basri G., Kuhi L.V., 1984, ApJ 277, 725
Chelli A., Cruz-Gonzalez I., Salas L., et al., 1997, Modulated temporal variability in DF Tauri: a bipolar Brγ emission structure. In: Malbet F., Castet A. (eds.) Poster Proceeding of the IAU Symposium 182. Chamonix (France), 263
Gullbring E., Hartmann L., Briceño C., Calvet N., 1998, ApJ 492, 323
Hartigan P., Hartmann L., Kenyon S.J., Hewett R., Stauffer J., 1989, ApJS 70, 899
Hartigan P., Kenyon S.J., Hartmann L., et al., 1991, ApJ 382, 617
Hartmann L., Kenyon S.J., 1990, ApJ 349, 160
Hartmann L., Hewett R., Calvet N., 1994, ApJ 426, 669
Herbig G.H., Bell K.R., 1988, Lick Obs. Bull. 1111
Knoechel G., Von der Heide K., 1978, A&A 67, 209
Lynden-Bell D., Pringle J.E., 1974, MNRAS 168, 603
Papoulis A., 1965, Probability, Random Variables and Stochastic Processes. McGraw Hill, New York, p. 212
Walker M.F., 1987, PASP 99, 392